

W and Z Production in the Forward Region with LHCb

Philip Ilten
on behalf of the LHCb Collaboration

Department of Physics, University College Dublin

Abstract. Results for W and Z boson production from pp collisions at $\sqrt{s} = 7$ TeV in the LHCb experiment are presented. Due to LHCb's unique forward acceptance in pseudorapidity of $2.0 \leq \eta \leq 4.5$ these results are a test of the Standard Model in the forward region, and can be used to better constrain parton density functions in the low x kinematic regime.

Keywords: electroweak, LHCb, LHC

PACS: 13.38.-b, 13.35.Dx

INTRODUCTION

The LHCb detector is a fully instrumented forward arm spectrometer at the LHC, purpose built for B -hadron physics [1]. Due to the forward acceptance of the detector, $2.0 \leq \eta \leq 4.5$, LHCb provides unique and complimentary precision electroweak measurements to the pseudorapidity range of the CMS and ATLAS detectors, $|\eta| < 2.5$.

Partonic cross sections for W and Z production can be calculated using NNLO electroweak theory to a precision of one percent. However, PDF distributions introduce an additional uncertainty in the observable hadronic cross sections at the LHC. The hadronic uncertainty is dependent upon the rapidity of the electroweak boson, increasing for larger rapidities. For $y < 2$ an uncertainty of $\approx 1\%$ is introduced, whereas for $y \approx 5$ the uncertainty increases to $\approx 8\%$ [2]. Additionally, the expected sign change in W^\pm charge asymmetry falls inside LHCb acceptance. Within this review the Z and W cross sections measured at LHCb are summarised for $W \rightarrow \mu$ and $Z \rightarrow \mu\mu$ with $37.1 \pm 1.3 \text{ pb}^{-1}$ of data, $Z \rightarrow \tau\tau \rightarrow \mu e$ with $247.9 \pm 12.7 \text{ pb}^{-1}$ of data, and $Z \rightarrow \tau\tau \rightarrow \mu e$ with $246.4 \pm 12.6 \text{ pb}^{-1}$ of data (neutrinos are omitted in the notation for brevity) [3, 4].

W SELECTION

For the $W \rightarrow \mu$ selection a single muon with $p_T > 20$ GeV and $2.0 \leq \eta \leq 4.5$ is used. Two light flavour QCD backgrounds are considered, decay in flight and punch through of pions and kaons. These backgrounds are reduced by requiring the summed p_T of all tracks and photons within a cone of $\Delta R \equiv \sqrt{\Delta\phi^2 + \Delta\eta^2} < 0.5$ to be less than 2 GeV and the sum of the associated electromagnetic and hadronic calorimeter energies over the track momentum to be less than 0.04. Requiring the muon impact parameter to be less than $40 \mu\text{m}$ minimises heavy flavour QCD backgrounds and requiring no additional muons with $p_T > 5$ GeV in the event suppresses electroweak backgrounds.

The signal and background composition of the observed events is determined using a template fit where the $W \rightarrow \mu$ and QCD decay in flight template shapes are allowed to float. Electroweak background shapes are calculated using POWHEG [5] and Pythia [6] and normalised to the observed cross sections. The QCD and heavy flavour shapes are determined from data and, excepting QCD decay in flight, normalised using simulation. The final template fit is performed over lepton p_T and shown in Figure 1a. Further details on background estimation can be found in Reference [3].

Z SELECTION

The $Z \rightarrow \mu\mu$ selection requires two opposite sign muons of $p_T > 20$ GeV with $2.0 \leq \eta \leq 4.5$ and an invariant mass, shown in Figure 1b, between $60 \leq M_{\mu\mu} \leq 120$ GeV. The QCD background is estimated from same sign events, while the heavy flavour background shape is determined from data and normalised using simulation. The $Z \rightarrow \tau\tau$ background is taken from simulation.

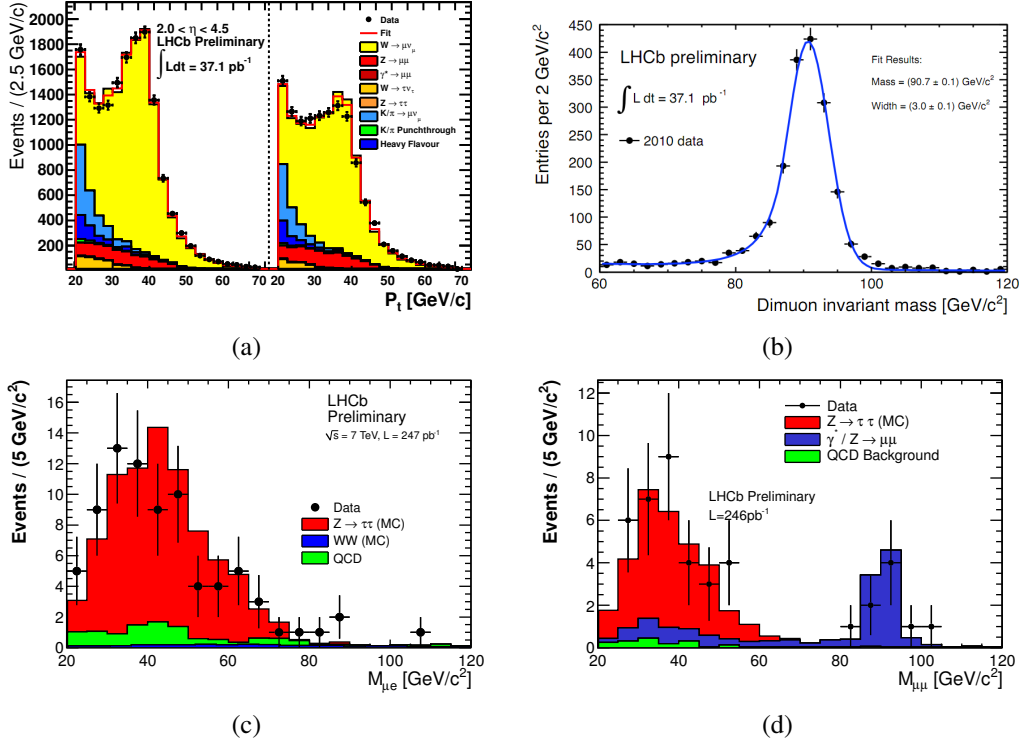


FIGURE 1. Transverse momentum distribution for the W^+ (left) and W^- (right) (a), and the dilepton invariant masses for $Z \rightarrow \mu\mu$ (b), $Z \rightarrow \tau\tau \rightarrow \mu e$ (c), and $Z \rightarrow \tau\tau \rightarrow \mu\mu$ (d).

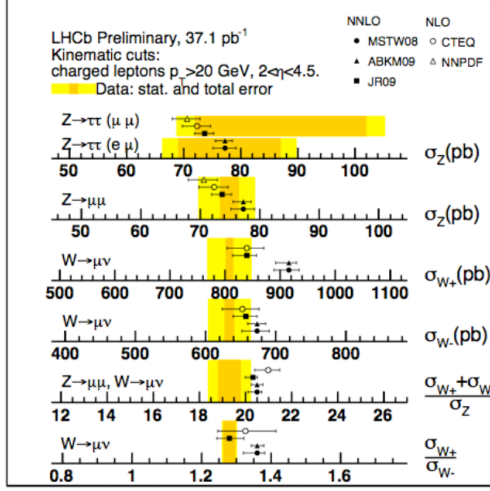
For the $Z \rightarrow \tau\tau \rightarrow \mu e$ and $Z \rightarrow \tau\tau \rightarrow \mu\mu$ selections a muon with $p_T > 20$ and opposite sign electron (or muon) with $p_T > 5$ GeV are required in $2.0 \leq \eta \leq 4.5$ with dilepton invariant mass, Figures 1c and 1d, greater than 20 GeV. The p_T of all tracks within a cone of $\Delta R < 0.5$ around the leptons is summed and the minimum isolation asymmetry of the two leptons, $(p_\ell - \sum p_{\text{track}})/(p_\ell + \sum p_{\text{track}})$, must be greater than 0.8 to reduce QCD background. The $t\bar{t}$ and WW backgrounds are suppressed by an acoplanarity cut on the two leptons, $\Delta\phi > 2.7$. For the $Z \rightarrow \tau\tau \rightarrow \mu\mu$ channel, cuts on the summed impact parameter significance of the two leptons, $\sum \text{IP} > 4$, the p_T asymmetry of the two muons, $(p_T^{\mu_1} - p_T^{\mu_2})/(p_T^{\mu_1} + p_T^{\mu_2}) > 0.2$, and the dilepton invariant mass, $M_{\mu\mu} < 80$ GeV, reduce the $\gamma^*/Z \rightarrow \mu\mu$ background.

The QCD and γ^*/Z backgrounds are estimated from data, while the $t\bar{t}$ and WW backgrounds are calculated using simulation. Further details on background estimation are available in Reference [4].

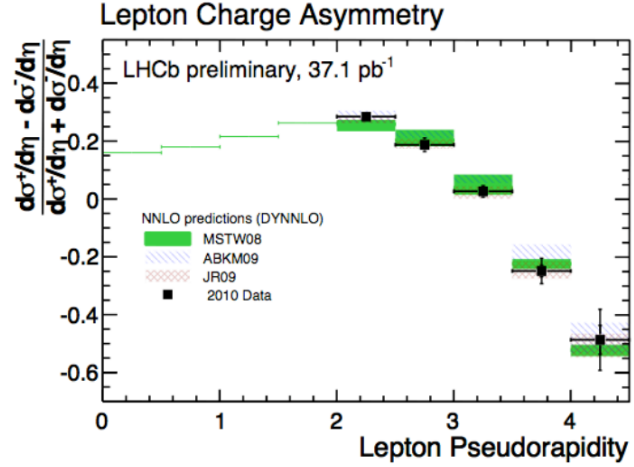
CROSS SECTIONS

The W and Z cross sections are defined as $\sigma(2.0 \leq \eta^{\mu, \ell} \leq 4.5, p_T^{\mu, \ell} > 20 \text{ GeV}) = (N - N_{\text{bkg}})/(A\epsilon_{\text{tot}}\mathcal{L}BR)$, where N is total number of events, N_{bkg} is number of background events, A is acceptance, \mathcal{L} is integrated luminosity, BR is the branching ratio for the process, and ϵ_{tot} is the total efficiency. The Z total efficiency is split into $\epsilon_{\text{tot}}^Z = A^Z \epsilon_{\text{trk}}^{\mu} \epsilon_{\text{trk}}^{\ell} \epsilon_{\text{id}}^{\mu} \epsilon_{\text{id}}^{\ell} \epsilon_{\text{sel}}^Z$, while the W total efficiency is split into $\epsilon_{\text{tot}}^W = A^W \epsilon_{\text{trg}}^{\mu} \epsilon_{\text{id}}^{\mu} \epsilon_{\text{sel}}^W$. The trigger efficiencies are calculated from the $Z \rightarrow \mu\mu$ data. The muon track and identification efficiencies are calculated using a tag and probe method on the $Z \rightarrow \mu\mu$ data while the electron identification efficiency uses a $Z \rightarrow ee$ data sample. The electron track efficiency is estimated from simulation and data. The $Z \rightarrow \mu\mu$ selection efficiency is unity by definition and the $W \rightarrow \mu$ selection efficiency is found from $Z \rightarrow \mu\mu$ events. Both the $Z \rightarrow \tau\tau \rightarrow \mu e$ and $Z \rightarrow \tau\tau \rightarrow \mu\mu$ selection efficiencies are calculated from simulation and data. The uncertainties for efficiencies from data are statistical, while the data and simulation efficiency uncertainties are taken as the difference between simulation and data.

The $Z \rightarrow \mu\mu$ and $W \rightarrow \mu$ acceptances are defined as unity, while the $Z \rightarrow \tau\tau$ acceptances are calculated using both Pythia and Herwig++ [7] with uncertainty estimated from the difference. The observed cross sections corrected for



(a)



(b)

FIGURE 2. A summary of the total cross section measurements (a) and the measured W^\pm charge asymmetry (b).

FSR [8] are,

$$\begin{aligned} \sigma_{W^+ \rightarrow \mu^+} &= 808 \pm 7 \pm 28 \pm 28, & \sigma_{W^- \rightarrow \mu^-} &= 634 \pm 7 \pm 21 \pm 22, & \sigma_{Z \rightarrow \mu\mu} &= 74.9 \pm 1.6 \pm 3.8 \pm 2.6 \\ \sigma_{Z \rightarrow \tau\tau \rightarrow \mu\mu} &= 89 \pm 15 \pm 10 \pm 5, & \sigma_{Z \rightarrow \tau\tau \rightarrow \mu e} &= 79 \pm 9 \pm 8 \pm 4 \end{aligned} \quad (1)$$

in pb, where the first uncertainty is statistical, the second uncertainty is systematic estimated from background, efficiency, and acceptance uncertainty, and the third is luminosity uncertainty. A comparison of the cross sections to NLO theory from MCFM [9] and FEWZ [10] using the CTEQ [11] and NNPDF [12] PDF sets and NNLO theory from DYNNLO [13] using the MSTW08 [2], ABKM09 [14], and JR09 [15] PDF sets is given in Figure 2a while the differential W^\pm asymmetry is given in Figure 2b.

CONCLUSION

Cross sections in the forward region, $2.0 \leq \eta \leq 4.5$, have been presented for $W \rightarrow \mu$, $Z \rightarrow \mu\mu$, $Z \rightarrow \tau\tau \rightarrow \mu\mu$, and $Z \rightarrow \tau\tau \rightarrow \mu e$ processes and agree well with NLO predictions. The differential W^\pm charge asymmetry has been measured and matches NLO and NNLO predictions. The continuation of these analyses will help further constrain PDF's and reduce their uncertainties at low x .

ACKNOWLEDGMENTS

Copyright CERN for the benefit of the LHCb Collaboration.

REFERENCES

1. The LHCb Collaboration, *Journal of Instrumentation* **3** (2008).
2. A. Martin, W. Stirling, R. Thorne, and G. Watt, *Eur.Phys.J.* **C63**, 189–285 (2009).
3. The LHCb Collaboration (2011), LHCb-CONF-2011-039.
4. The LHCb Collaboration (2011), LHCb-CONF-2011-041.
5. P. Nason, *JHEP* **0411**, 040 (2004).
6. T. Sjostrand, S. Mrenna, and P. Z. Skands, *JHEP* **0605**, 026 (2006).
7. M. Bahr, S. Gieseke, M. Gigg, D. Grellscheid, K. Hamilton, et al., *Eur.Phys.J.* **C58**, 639–707 (2008).
8. C. Carloni Calame, G. Montagna, O. Nicrosini, and M. Treccani, *Phys.Rev.* **D69**, 037301 (2004).

9. J. M. Campbell, and R. Ellis, *Nucl.Phys.Proc.Suppl.* **205-206**, 10–15 (2010).
10. R. Gavin, Y. Li, F. Petriello, and S. Quackenbush, *Comput.Phys.Commun.* **182**, 2388–2403 (2011).
11. P. M. Nadolsky, H.-L. Lai, Q.-H. Cao, J. Huston, J. Pumplin, et al., *Phys.Rev.* **D78**, 013004 (2008).
12. R. D. Ball, L. Del Debbio, S. Forte, A. Guffanti, J. I. Latorre, et al., *Nucl.Phys.* **B838**, 136–206 (2010).
13. S. Catani, and M. Grazzini, *Phys.Rev.Lett.* **98**, 222002 (2007).
14. S. Alekhin, J. Blumlein, S. Klein, and S. Moch, *Phys.Rev.* **D81**, 014032 (2010).
15. P. Jimenez-Delgado, and E. Reya, *Phys.Rev.* **D79**, 074023 (2009).